Electric-field-induced adiabaticity in the rovibrational motion of heteronuclear diatomic molecules

R. González-Férez[1,*] and P. Schmelcher[2,3,†]
[1]*Departamento de Física Moderna and Instituto "Carlos I" de Física Teórica y Computacional, Universidad de Granada, E-18071 Granada, Spain*
[2]*Theoretische Chemie, Physikalisch-Chemisches Institut, Im Neuenheimer Feld 229, D-69120 Heidelberg, Germany*
[3]*Physikalisches Institut, Universität Heidelberg, Philosophenweg 12, D-69120 Heidelberg, Germany*
(Received 26 November 2004; published 24 March 2005)

We investigate the rovibrational dynamics of heteronuclear diatomic molecules exposed to a strong external static and homogeneous electric field. We encounter in the presence of the field the effect of induced adiabatic coupling among the vibrational and hybridized rotational motions. Exact results are compared to the predictions of the adiabatic rotor approach as well as to the previously established effective rotor approximation. A detailed analysis of the impact of the electric field is performed: the hybridized and oriented rotational motion, the mixing of angular momenta, and the squeezing of the vibrational motion are observed. It is demonstrated that these effects can well be accounted for by the adiabatic rotor approximation.

DOI: 10.1103/PhysRevA.71.033416 PACS number(s): 33.80.Ps, 33.55.Be, 33.20.Vq

I. INTRODUCTION

Molecules exposed to external fields represent, in spite of its substantial history, a very active and promising research area with several intriguing perspectives. Due to the key role that external fields play in the cooling, trapping, and guiding of atoms and molecules, the availability of molecular Bose-Einstein condensates [1–3] has stimulated further studies. Indeed, the long-range anisotropic dipole-dipole interaction between ultracold polar molecules will give rise to interesting physics, such as cold molecule-molecule collision dynamics [4–7], molecular collective quantum effects [8,9], ultrahigh resolution and high-precision spectroscopy, chemical reactions [10,11], molecular optics and interferometry, and potentially also to quantum computing [12]. Moreover, the availability of ultracold molecules might provide an improvement of the precision of several experiments involving molecules, such as the measurement of the dipole moment of the electron [13,14], the measurement of the time variation of the fine-structure constant [15], or the study of weak interaction effects in chiral molecules [16].

In particular, electric fields play an important role in one of the main experimental techniques to trap molecules. An array of time varying inhomogeneous electric fields has been used to decelerate and trap polar molecules [17,18], providing a different technique which can be used for a large variety of neutral molecules. Recently, the control of the translational motion of Rydberg states of the H_2 molecule has been demonstrated by applying an inhomogeneous electric field [19]. The group of Bohn has introduced an uncommon species of molecular states called "field linked" states [20,21] which are composed of two ground-state polar molecules held at large internuclear separation under the joint influence of electric dipole forces and external electric fields. They have shown how the main properties of these states strongly depend on the external electric field, leading to control over the ultracold scattering properties [20,21].

Initially studies of molecules in electric fields were motivated by the possibility to get a deeper insight into chemical reaction dynamics by controlling the orientation or alignment of the involved molecules. At the end of the 1970s the orientation of symmetric top molecules with permanent electric dipole moments was achieved by using a hexapole electric field [22,23]. Only molecules in a few specific preselected states could be oriented this way. In the early 1990s the orientation of molecules in Σ states became possible via the passage of the corresponding molecules through an electric field, known as the "brute force" method [24]. Strong electric fields have subsequently been used to orient the rotational motion of diatomic and also of polyatomic molecules [24–29]. In the beginning only static electric fields were employed and low-lying rotational states were considered. Subsequently also magnetic fields [30] were used to orient paramagnetic molecules [31] and more recently intense laser fields have been employed to align molecules [32–36].

Traditionally the theoretical description of the nuclear dynamics of molecules in an electric field is based on the rigid rotor approximation [37], neglecting the "coupling" between the vibrational and rotational motions and assuming a permanent dipole moment for the molecule. The pendular states appear for strong electric field when the molecule is oriented along the field direction and the rotational motion becomes a librating one, each pendular state being a coherent superposition of field-free rotational states [38]. It is only recently that the authors provided a full rovibrational description (FRV) of a heteronuclear diatomic molecule in a homogeneous electric field including the coupling between the vibrational and rotational motions and taking into account that the electric dipole moment functions depend on the internuclear coordinate [39]. An effective rotor approximation (ERA) which describes the effect of the electric field on rigid diatomic molecules [39] was developed. The ERA includes

*Electronic address: rogonzal@ugr.es
†Electronic address: Peter.Schmelcher@pci.uni-heidelberg.de

main properties of each vibrational state, and it has been shown to describe the effect of the electric field even for highly excited rovibrational states of the molecule, being superior to the traditional rigid rotor approach.

In the present work we go beyond the regime of validity of the effective rotor approach which represents a crude adiabatic approximation with respect to the separation of the vibrational and rotational motion. In particular we investigate the regime for which a fully adiabatic separation of the rovibrational motion is necessary: the fast vibrational motion depends now parametrically on the angular coordinates. The latter effect is exclusively due to the presence of the external electric field. Since we focus on effects due to the field-induced adiabaticity and their theoretical description in general we refrain from using potential-energy curves and dipole moment functions belonging to specific molecules but use parameter-dependent models of them in order to address and cover as many as possible physically different situations. The use of these models does not affect the general validity of our results. We address the regime of field strengths for which a nonperturbative description of the nuclear motion is necessary assuming that the effects of the electric field on the electronic motion can be described perturbatively.

The paper is organized as follows. In Sec. II we define our rovibrational Hamiltonian and we briefly discuss some specifics of our computational method. Here we also present the key aspects of the adiabatic separation of the vibrational and rotational motions in order to obtain the adiabatic rotor Hamiltonian. In Sec. III we describe the potential-energy curves and electric dipole moment functions used to model a general heteronuclear diatomic molecule. In Sec. IV we present the results and their discussion, including a detailed comparison of the adiabatic rotor approach (ARA) with the full rovibrational description. The conclusions and outlook are provided in Sec. V. Atomic units will be used throughout, unless stated otherwise.

II. ROVIBRATIONAL HAMILTONIAN AND THE ADIABATIC ROTOR APPROXIMATION

We employ the Born-Oppenheimer approximation for the Hamiltonian of a heteronuclear diatomic molecule which is assumed to be in its $^1\Sigma^+$ electronic ground state. The molecule is exposed to an external homogeneous and static electric field. In the rotating molecule fixed frame with the coordinate origin at the center of mass of the nuclei the Hamiltonian describing the nuclear motion takes on the following appearance:

$$\mathcal{H} = -\frac{\hbar^2}{2\mu R^2}\frac{\partial}{\partial R}\left(R^2\frac{\partial}{\partial R}\right) + \frac{\mathbf{J}^2(\theta,\phi)}{2\mu R^2} + \varepsilon(R) - FD(R)\cos\theta, \tag{1}$$

where R and θ,ϕ are the internuclear coordinate and Euler angles, respectively, and μ is the reduced mass of the nuclei. $\mathbf{J}(\theta,\phi)$ is the orbital angular momentum, $\varepsilon(R)$ represents the electronic potential-energy curve (PEC) of the molecule in field-free space, and $D(R)$ is the corresponding electronic dipole moment function (EDMF). The first and second terms are the vibrational and rotational kinetic energies, and the last term provides the interaction with an electric field of strength F, which is oriented parallel to the z axis of the laboratory frame. As it was stated above, we consider the regime where perturbation theory holds for the description of the electronic structure but a nonperturbative treatment is indispensable for the corresponding nuclear dynamics.

In the field-free case each state is characterized by its vibrational ν, rotational J, and magnetic M quantum numbers. In particular, the exact solution to the Schrödinger equation belonging to the Hamiltonian (1) is a product of a purely R-dependent vibrational wave function that depends parametrically on the conserved angular momentum J and a spherical harmonic depending exclusively on the angles θ,ϕ. In the presence of an external electric field only the magnetic quantum number M is conserved, giving rise to a nonintegrable two-dimensional dynamics in (R,θ) space. In order to solve the corresponding rovibrational equation of motion we use a hybrid computational approach, which combines discrete and basis-set methods. For the angular part a basis-set expansion in terms of associated Legendre polynomials is used, taking into account that M is conserved. The vibrational degree of freedom is treated by a discrete variable representation. Due to the typical shape of the molecular PEC, we choose the radial harmonic oscillator discrete variable representation, where the odd harmonic oscillator functions are taken as basis functions. Employing the variational principle, the initial differential equation is finally reduced to a symmetric eigenvalue problem which is diagonalized with the help of Krylov space techniques.

The theoretical description of the angular motion of a diatomic molecule in an external field is traditionally based on the rigid rotor approach for which the so-called pendular Hamiltonian reads

$$\mathcal{H} = \frac{\mathbf{J}^2}{2\mu R_{\mathrm{eq}}^2} - FD_{\mathrm{eq}}\cos\theta, \tag{2}$$

where R_{eq} and D_{eq} are the equilibrium internuclear distance and the corresponding dipole moment, respectively. For diatomic molecules this rigid rotor Hamiltonian is integrable and it was solved numerically in the seventies by von Meyenn [37]. Recently, the authors went beyond this rigid rotor description and proposed an effective rotor approximation which includes the main characteristics of each vibrational state [39]. The corresponding effective rotor Hamiltonian reads as follows:

$$\mathcal{H}_\nu^{\mathcal{R}} = \frac{1}{2\mu}\langle R^{-2}\rangle_\nu^{(0)}\mathbf{J}^2 - F\langle D(R)\rangle_\nu^{(0)}\cos\theta + E_\nu^{(0)} \tag{3}$$

with $\langle R^{-2}\rangle_\nu^{(0)} = \langle\psi_\nu^{(0)}|R^{-2}|\psi_\nu^{(0)}\rangle$, $\langle D(R)\rangle_\nu^{(0)} = \langle\psi_\nu^{(0)}|D(R)|\psi_\nu^{(0)}\rangle$, and $\psi_\nu^{(0)}$ and $E_\nu^{(0)}$ are the field-free vibrational wave function and energy, respectively. The total wave functions for the nuclear motion are $\psi_\nu^{(0)}(R)\cdot\chi_\kappa(\theta)$ where χ_κ are the eigenfunctions of the Hamiltonian (3). The ERA takes into account the vibrational state dependent moment of inertia and the dependence of the electric dipole moment on the vibrational coordinate, which are of particular importance for highly excited vibrational states. It was shown to properly describe both low-

lying and highly excited rovibrational states exposed to an electric field. In particular it is superior to the traditional rigid rotor approach [39].

The effective rotor represents, in the terminology of an adiabatic approach, a crude adiabatic approximation to the true wave function thereby neglecting the influence of the electric field on the vibrational motion. Obviously, this approximation is expected not to hold for arbitrary parameters and regimes, i.e., for arbitrary excitations, field strengths, and molecular species. In the present work we investigate the rovibrational motion in a regime where the vibrational motion is modified by the electric field, i.e., it becomes parametrically dependent on the slow angular variable θ. This leads to interesting effects in the rovibrational spectra and eigenfunctions which occur typically in the strong-field regime.

Following Ref. [39] we exploit the conservation of the angular momentum associated with the angular motion due to ϕ by the ansatz $\Psi(R,\theta,\phi)=\Psi_M(R,\theta)e^{iM\phi}$, with M being the magnetic quantum number. We restrict ourselves to the case $M=0$. Let us now perform an adiabatic separation of the vibrational and rotational motion. To this end we assume that the vibrational problem has been solved for a specific value of the rotational coordinate θ,

$$\left[-\frac{\hbar^2}{2\mu R^2}\frac{\partial}{\partial R}\left(R^2\frac{\partial}{\partial R}\right)+\epsilon(R)-FD(R)\cos\theta\right]\psi_\nu(R;\theta) = E_\nu(\theta)\psi_\nu(R;\theta), \tag{4}$$

where $\psi_\nu(R;\theta)$ is a member of the orthonormal vibrational eigenfunctions labeled by ν. $\psi_\nu(R;\theta)$ depends parametrically on the angle θ. Making the following ansatz for the rovibrational wave function:

$$\Psi(R,\theta)=\sum_\nu \psi_\nu(R;\theta)\chi_\nu(\theta),$$

and inserting it in the rovibrational equation of motion belonging to the Hamiltonian (1), after left multiplication with $\psi_\nu^*(R;\theta)$, and performing the integral over R, using the orthonormality of the vibrational adiabatic eigenfunctions as well as Eq. (4) we arrive at

$$\left[\frac{1}{2\mu}\langle R^{-2}\rangle_\nu \mathbf{J}^2+E_\nu(\theta)-E\right]\chi_\nu(\theta)+\sum_\kappa\left(\frac{A^2_{\nu\kappa}}{2}+A^1_{\nu\kappa}\mathbf{J}\right)\chi_\kappa(\theta) + \sum_{\kappa\neq\nu}\frac{A^0_{\nu\kappa}}{2}\mathbf{J}^2\chi_\kappa(\theta)=0 \tag{5}$$

with

$$\langle R^{-2}\rangle_\nu=\int_0^\infty \psi_\nu^*(R;\theta)\psi_\nu(R;\theta)dR,$$

$$A^j_{\nu\kappa}=\frac{1}{\mu}\int_0^\infty \psi_\nu^*(R;\theta)\mathbf{J}^j\psi_\kappa(R;\theta)dR,\quad j=0,1,2, \tag{6}$$

where $A^j_{\nu\kappa}$ are nonadiabatic coupling terms involving different vibrational eigenfunctions, $E_\nu(\theta)$ represents a potential for the motion in θ space, and $(1/2\mu)\langle R^{-2}\rangle_\nu\mathbf{J}^2$ is an effective rotational kinetic energy. If the nonadiabatic coupling elements are neglected Eq. (5) reduces to a single channel equation and an adiabatic separation and approximation of the angular and radial motions has been achieved.

Let us comment on the vibrational equation of motion (4). For weak electric fields the interaction term $-FD(R)\cos\theta$ is significantly smaller than the vibrational spacing due to the electronic PEC. This allows us to use the field-free vibrational wave functions and to apply first-order perturbation theory (see Ref. [39]) with respect to the electric-field terms thereby leading to the effective rotor Hamiltonian (3). However, for sufficiently strong electric fields and/or highly excited vibrational states, the interaction with the electric field leads vibrational states that depend parametrically on the angular variable θ. We therefore enter a regime for which the above adiabatic separation still holds but the vibrational motion is affected by the electric field. In practice one then solves the vibrational equation of motion (4) on an angular grid, $\{\theta_i,\ i=1,\ldots,N\}$ thereby obtaining $\psi_\nu(R;\theta_i)$ and $E_\nu(\theta_i)$. This allows us to compute the expectation values $\langle\psi_\nu(R;\theta_i)|R^{-2}|\psi_\nu(R;\theta_i)\rangle$ and in principal also the nonadiabatic coupling elements $A^j_{\nu\kappa}$ which both depend on θ.

Here we assume the validity of the adiabatic approximation to the separation of the vibrational and rotational motion and neglect all nonadiabatic coupling elements. This defines the "adiabatic rotor approach" and the "adiabatic rotor Hamiltonian" describing the rotational motion of the molecular system:

$$\left[\frac{1}{2\mu}\langle R^{-2}\rangle_\nu\mathbf{J}^2+E_\nu(\theta)-E\right]\chi_\nu(\theta)=0, \tag{7}$$

where the first term is an effective rotational kinetic energy and the second one represents the interaction with the electric field. The rotational equation of motion (7) looks different for each vibrational state since it explicitly contains the expectation values $\langle R^{-2}\rangle_\nu$ and the vibrational energy $E_\nu(\theta)$, which have to be computed for each state.

The main difference of the adiabatic rotor approximation (7) compared to the previously obtained effective rotor approach (3) is the way the vibrational motion is treated. The expression (7) takes into account the influence of the electric field on the vibrational motion, which might be of importance for very strong electric fields or highly excited vibrational levels due to the field-induced adiabatic coupling between the rotational and vibrational motions. In contrast to this we neglected the influence of the electric field on the vibrational motion in case of the effective rotor approach. Obviously, the effective rotor approach is contained in the adiabatic rotor approach. Both approximations are, however, complementary in the following sense. There is a large number of situations depending on the field strength, the EDMF, and on the part of the spectrum under consideration, where either the ERA or the ARA might be sufficient to describe the behavior and properties in the field.

Let us comment on how to solve the resulting equations (4) and (7) of the above scheme. In a first step, and in order to facilitate the computational procedure, we choose the zeros of the N_Rth order associated Legendre polynomial as grid

points for the angular coordinate. The vibrational equation (4) is integrated with the help of the discrete variable approach N_R times on the grid $\{\theta_i\}$, thus we obtain the vibrational wave functions $\psi_\nu(R;\theta_i)$ and the corresponding spectrum $E_\nu(\theta_i)$. The expectation value $\langle R^{-2}\rangle_\nu$ is computed. These quantities, $E_\nu(\theta_i)$ and $\langle R^{-2}\rangle_\nu$, are introduced in the effective rotational equation of motion (7), which is solved by means of a basis-set expansion with respect to the associated Legendre polynomials.

There are two reasons for applying the adiabatic rotor approximation compared to the full rovibrational description of the problem. First, a fully adiabatic approach describes emerging field-induced effects. Second, from a computational point of view it provides a drastic reduction of the numerical effort. In both cases we need the same number of grid points N_V in the discrete variable representation applied to the vibrational coordinate, and the same number of angular functions N_R in the basis-set expansion performed for the rotational coordinate. In the full rovibrational description we have to diagonalize a $N\times N$ real symmetric banded eigenvalue problem with $N=N_V\cdot N_R$. However, in the case of the ARA we first diagonalize N_R times a $N_V\times N_V$ real symmetric banded eigenvalue problem for the vibrational part and subsequently for each vibrational state an $N_R\times N_R$ real symmetric eigenvalue problem to diagonalize the rotational equation of motion.

III. POTENTIAL-ENERGY CURVE AND ELECTRONIC DIPOLE MOMENT FUNCTION

The electronic potential-energy curves and the electronic dipole moment functions provide valuable information on the properties of a molecular system including its rovibrational spectrum and its response to external fields. Both quantities can be obtained from *ab initio* calculations and/or experimental results in the literature. Since we are interested in predicting general properties and principal effects with the focus on their understanding and theoretical description we do not address a specific molecular system but use model functions for the PEC and the EDMF.

As a PEC we employ the Morse potential

$$\varepsilon(R) = d_e\left[e^{-2\alpha(R-R_e)} - 2e^{-\alpha(R-R_e)}\right], \tag{8}$$

where R_e and d_e are the equilibrium internuclear distance and the depth of the potential well, respectively. Here we choose the values $\alpha=0.5$, $d_e=0.02$, and $R_e=6.0$ a.u. being motivated by the shape of the PEC of heteronuclear alkali dimers [40]. The latter are characterized by a large equilibrium distance $R_e\sim 6-7$ a.u., and a very shallow potential well. We will also study the case $\alpha=0.5$, $d_e=0.02$, and $R_e=2.2$ a.u. We remark that our model potential does not possess the correct asymptotic behavior for large R which is of importance for very high excitations close to the dissociation threshold. Our investigation therefore focuses on not too high excitations for which the asymptotics is irrelevant.

In order to illustrate the difference with respect to the energy scales of the vibrational and rotational motions we have computed the vibrational and rotational energy spacing for a vanishing electric field. The rotational and vibrational spacing are $\Delta E_r^\nu = E_{\nu,1} - E_{\nu,0}$ and $\Delta E_v^\nu = E_{\nu+1,0} - E_{\nu,0}$, respectively, with $E_{\nu,J}$ being the field-free energy of the (ν,J) state. Figure 1 presents these two quantities as a function of the vibrational quantum number $0\leqslant\nu\leqslant 20$ for the PECs with $R_e=2.2$ a.u. and $R_e=6$ a.u. Note that the vibrational spacing is independent of the equilibrium distance R_e, and the difference between both sets of parameters is due to the rotational spacing. For the Morse potential with $R_e=2.2$ a.u. the ratio between both quantities takes the initial value $\Delta E_v^0/\Delta E_r^0 \approx 53$, and it decreases monotonically as ν is increased, reaching for the highest state the value $\Delta E_v^{20}/\Delta E_r^{20}\approx 39$. For the Morse with $R_e=6.0$ a.u. a similar behavior is observed, although now the ratios are $\Delta E_v^0/\Delta E_r^0\approx 396$ and $\Delta E_v^{20}/\Delta E_r^{20} \approx 319$, i.e., almost one order of magnitude larger than in the previous case. It is clear from these results that the energy scales associated with the rotational and vibrational motions are well separated.

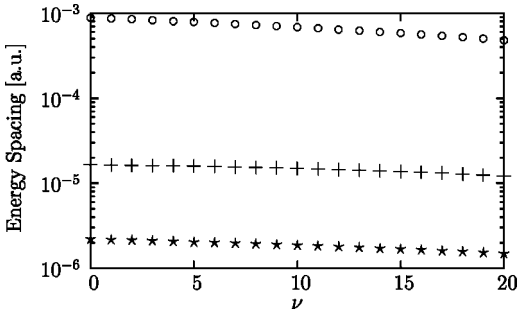

FIG. 1. Field-free vibrational energy spacings (○) for the Morse potentials with $R_e=2.2$ a.u. and $R_e=6.0$ a.u. as a function of the vibrational quantum number ν. Field-free rotational energy spacings for the Morse with $R_e=2.2$ a.u.(+) and $R_e=6.0$ a.u.(⋆) as a function of the vibrational quantum number ν.

For the EDMF we take a Gaussian function given by

$$D(R) = M_0 e^{-A(R - R_e - \Delta)^2}, \tag{9}$$

where R_e is the equilibrium distance, A provides the width of the Gaussian, Δ is a shift with respect to R_e, and M_0 determines the strength of the EDMF at the maximum $R=R_e+\Delta$. By choosing this kind of function we ensure a proper asymptotic behavior of the EDMF, satisfying both $\lim_{R\to 0} D(R)=0$ and $\lim_{R\to\infty} D(R)=0$.

We have selected three different shapes for the EDMF, the main difference between them being the position of the maximum and the width of the Gaussian function. The chosen parameters are given in Table I. For the different appearances of the three functions we refer the reader to Fig. 2: D_C is centered at R_e, D_W is a broader function, its maximum

TABLE I. Parameters of the electric dipole moment functions; see text.

Name	M_0(D)	A (a.u.)	Δ (a.u.)
D_C	5	2	0
D_S	5	2	2
D_W	5	0.5	1

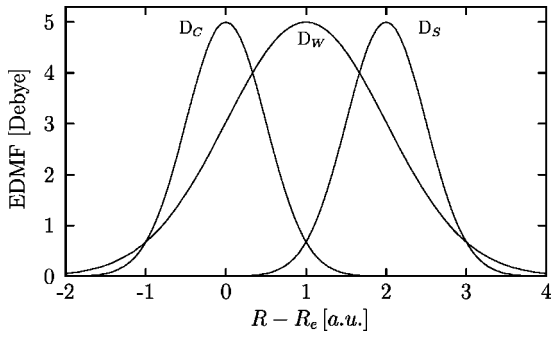

FIG. 2. The electric dipole moment functions used in our computations, centered D_C, shifted D_S, and wider D_W as a function of $R-R_e$.

being shifted with respect to R_e, and D_S is an even further shifted but again narrower dipole moment function. In many cases the electric dipole moment of heteronuclear diatomic molecules is a single humped function possessing its maximum at a position close to R_e. However, exceptions do occur such as the double humped dipole momentum function of the CO molecule that possesses a zero close to R_e and a broad outer hump for large internuclear distances.

IV. RESULTS AND COMPARISON OF THE ADIABATIC ROTOR APPROXIMATION WITH THE FULL ROVIBRATIONAL DESCRIPTION

We have performed a full rovibrational analysis [i.e., we solved the Schrödinger equation belonging to Eq. (1)] of the effects of an electric field on the six models for molecular systems, i.e., the Morse with $R_e=2.2,6$ a.u., and the three EDMFs being centered (D_C), shifted (D_S), and widened (D_W). The reduced mass of the CO molecule $\mu=12\,498.102$ a.u. has been used. In order to show very well pronounced effects for our model system we will choose a field strength $F=10^{-3}$a.u. corresponding to 514 (MV/m) which is somewhat stronger than the static fields available in the laboratory. We emphasize, however, that the observed effects are expected to be pronounced for significantly lower (laboratory) field strengths for highly excited rovibrational states of certain species, such as the alkali dimers.

For each molecule, we have computed the states with $0\leqslant\nu\leqslant 20$ and angular momentum $J=0$ for $M=0$ corresponding to the first 21 vibrational states in the absence of the field. The expectation values $\langle\cos\theta\rangle,\langle\mathbf{J}^2\rangle$, and $\langle R\rangle$, together with density profiles of the eigenfunctions enable us to find and analyze relevant phenomena. Equally we perform for our model systems studies in the framework of the adiabatic rotor approach (ARA) and the effective rotor approach (ERA). A comparison between these three approaches (exact, ARA, ERA) allows us to conclude upon the validity of the different approximations. Let us introduce the relative difference between the results obtained in the ERA and ARA compared to the full rovibrational description of the problem:

$$\Delta A_\nu^{\mathcal{X}}=\frac{|A_\nu^{\mathcal{F}}-A_\nu^{\mathcal{X}}|}{A_\nu^{\mathcal{F}}}\quad\text{with }\mathcal{X}=\mathcal{E},\mathcal{A},\tag{10}$$

where $A_\nu^{\mathcal{F}}$ represents one of the expectation values mentioned above and the upper right index $\mathcal{F},\mathcal{E},\mathcal{A}$ refers to the exact, ERA, and ARA approach.

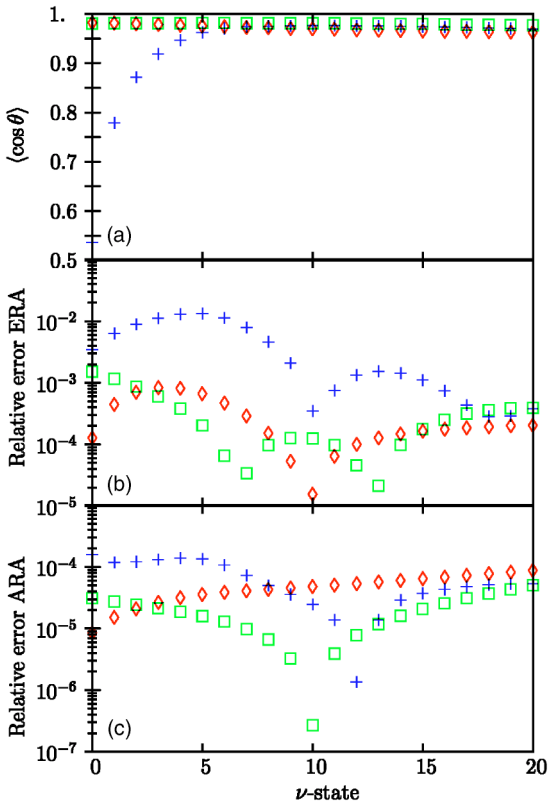

FIG. 3. (Color online) (a) The expectation values $\langle\cos\theta\rangle$, (b) the relative error $\Delta\langle\cos\theta\rangle_\nu^{\mathcal{E}}$ of the effective rotor approximation, (c) the relative error $\Delta\langle\cos\theta\rangle_\nu^{\mathcal{A}}$ of the adiabatic rotor approximation as a function of the vibrational label $0\leqslant\nu\leqslant 20$ for states emerging from $J=0$ for $F=0$ for the Morse potential with $R_e=6.0$ a.u. and the three EDMFs D_C (◇), D_S (+), and D_W (□).

In the following we will use ν and J as labels of the rovibrational states. These labels correspond to quantum numbers (conserved quantities) only in the case of the absence of the electric field whereas in the presence of the field a strong (rotation) and weak (vibration) mixing of field-free states takes place.

A. Morse potential for $R_e=6.0$ a.u.

Figure 3(a) shows the expectation values of $\langle\cos\theta\rangle$ for the rovibrational states with $0\leqslant\nu\leqslant 20$ emerging from the $J=0$ states for $F=0$ as a function of the vibrational number ν for the Morse potential with $R_e=6$ a.u. Results for the three Gaussian EDMF are included in this figure. $\langle\cos\theta\rangle$ provides a measure of the orientation of the molecule with respect to the field direction: the closer it is to 1, the stronger is the orientation. For D_C all states show a strong orientation, which slightly decreases as the degree of excitation is increased, from the rovibrational ground state with $\langle\cos\theta\rangle=0.9827$ to the $\nu=20$ state with $\langle\cos\theta\rangle=0.9626$. The behavior of the states in case of D_S is completely different. The effect of the electric field on the low-lying states is weak compared to the high-lying states. For the rovibrational ground state we have $\langle\cos\theta\rangle=0.5360$. The reason for this behavior is obviously the small values of D_S in the neighbor-

hood of the equilibrium internuclear distance. The orientation of the states increases as the vibrational number increases: It reaches a maximum for $\nu=10$ being $\langle\cos\theta\rangle=0.9761$ and slightly decreases thereafter. For D_W, $\langle\cos\theta\rangle$ increases very little with increasing ν and reaches a maximum for the state $\nu=5$ with $\langle\cos\theta\rangle=0.9813$. For $\nu=20$ we encounter $\langle\cos\theta\rangle=0.9766$. It is clear from Fig. 3 that the effects of the electric field on the orientation depend on the state under consideration but also strongly on the chosen EDMF. For these model systems and due to the strong electric-field strength all the considered states show a very strong orientation. In Fig. 3(b), the relative error for this expectation value computed by using the ERA, $\Delta\langle\cos\theta\rangle_\nu^{\mathcal{E}}$, is shown as a function of the vibrational number ν for the three EDMF. The results provided by the ERA for the expectation value $\langle\cos\theta\rangle$ for this molecule using the dipole moment functions D_C and D_W show a good agreement for all the states under consideration, i.e., we have $\Delta\langle\cos\theta\rangle_\nu^{\mathcal{E}}<0.01$ for $0\leqslant\nu\leqslant20$. Note, however, that in case of D_S the states for $\nu=2-5$ possess a relative error larger than 0.01, while for the remaining states $\Delta\langle\cos\theta\rangle_\nu^{\mathcal{E}}<0.01$. Figure 3(c) presents the relative error of $\langle\cos\theta\rangle$ using the ARA, $\Delta\langle\cos\theta\rangle_\nu^{\mathcal{A}}$, as a function of ν. Again all three cases of EDMF are considered. The results obtained for $\langle\cos\theta\rangle$ are excellent, i.e., $\Delta\langle\cos\theta\rangle_\nu^{\mathcal{A}}<2\times10^{-4}$ for all the states and any EDMF. Apart from a single exception ($\nu=10$) we have $\Delta\langle\cos\theta\rangle_\nu^{\mathcal{A}}\ll\Delta\langle\cos\theta\rangle_\nu^{\mathcal{E}}$ demonstrating that the adiabatic rotor approach is superior to the effective rotor one.

The dependence of the expectation value $\langle\mathbf{J}^2\rangle$ on the vibrational label ν is illustrated in Fig. 4(a) for the three EDMF. $\langle\mathbf{J}^2\rangle$ provides a measure for the mixture of the field-free angular momentum states with fixed M_J, i.e., it describes the hybridization of the rotational motion for $F=0$. The effects due to the electric field depend not only on the chosen EDMF but also strongly on the degree of excitation as already indicated when studying the corresponding behavior of $\langle\cos\theta\rangle$. For D_C, $\langle\mathbf{J}^2\rangle$ decreases significantly with increasing ν. All states show, however, a very strong hybridization of the rotational motion, i.e., $\langle\mathbf{J}^2\rangle=28.321$ for the rovibrational ground state and $\langle\mathbf{J}^2\rangle=12.872$ for the $\nu=20$ state. For D_W we encounter also a strong mixing: In this case $\langle\mathbf{J}^2\rangle$ slightly increases with ν reaching a maximum for $\nu=6$ with $\langle\mathbf{J}^2\rangle=26.229$ and decreasing thereafter. In case of D_S the low-lying states exhibit a much smaller hybridization compared to the previous cases: For the rovibrational ground state we find $\langle\mathbf{J}^2\rangle=0.527$. The reason for this effect is that the low-lying states "do not feel" the EDMF D_S, due to the small overlap of the wave function and the EDMF. In this case $\langle\mathbf{J}^2\rangle$ rapidly increases as ν increases, reaching a maximum for $\nu=10$ with $\langle\mathbf{J}^2\rangle=20.577$ and slightly decreases thereafter. Figure 4(b) shows the corresponding relative errors of this expectation value computed by means of the ERA, $\Delta\langle\mathbf{J}^2\rangle_\nu^{\mathcal{E}}$, as a function of the vibrational number ν. Note that for each EDMF there is a significant number of states with $\Delta\langle\mathbf{J}^2\rangle_\nu^{\mathcal{E}}>0.01$. Even more, for D_S the states with $\nu=3-8$ show $\Delta\langle\mathbf{J}^2\rangle_\nu^{\mathcal{E}}>0.1$. Therefore we can conclude that the ERA is not good enough to describe the hybridization of the rotational motion taking place in this systems. The relative errors for

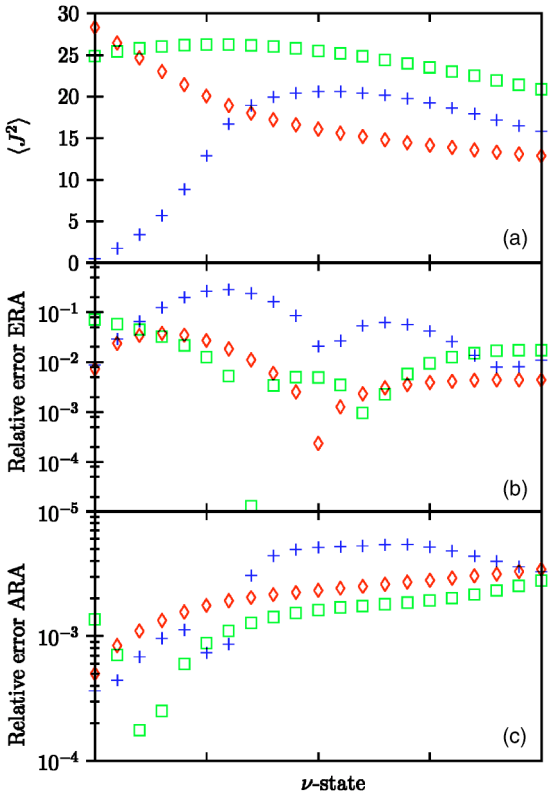

FIG. 4. (Color online) (a) The expectation values $\langle\mathbf{J}^2\rangle$, (b) the relative error $\Delta\langle\mathbf{J}^2\rangle_\nu^{\mathcal{E}}$ of the effective rotor approximation, (c) the relative error $\Delta\langle\mathbf{J}^2\rangle_\nu^{\mathcal{A}}$ of the adiabatic rotor approximation as a function of the vibrational label $0\leqslant\nu\leqslant20$ for states emerging from $J=0$ for $F=0$ for the Morse potential with $R_e=6.0$ a.u. and the three EDMFs D_C ($\diamond$), D_S (+), and D_W ($\square$).

the ARA, $\Delta\langle\mathbf{J}^2\rangle_\nu^{\mathcal{A}}$, as a function of ν are presented in Fig. 4(c). This figure clearly illustrates the advantage of our proposed approximation ARA compared to ERA. For the three EDMF and all the considered states we obtain relative errors significantly smaller than 0.01. We therefore conclude that the adiabatic rotor approach accurately describes the properties of the wave function whereas the effective rotor approximation fails to do so, at least in most cases.

To complete the description of the effect of the electric field on our systems, we illustrate in Fig. 5(a) the expectation value of the vibrational coordinate $\langle R\rangle$ as a function of ν for the same set of states and EDMF. For comparison also the corresponding field-free values of $\langle R\rangle$ have been included. This expectation value provides a measure of the size of the molecular state. In the case of D_C the states satisfy $\langle R\rangle^F<\langle R\rangle^0$, where F indicates the presence of the field and 0 stands for $F=0$. They are attracted towards the maximum of D_C at $R=6$ a.u. and have a lower energy compared to the field-free case. For the low-lying states, $\nu=0-2$, in the case of D_S we obtain $\langle R\rangle^F\approx\langle R\rangle^0$, the maximum of D_S at $R=8$ a.u. is too far, and therefore the attraction is not strong enough to modify the vibrational part of the wave function. The states $\nu=3-11$ show a completely different behavior, i.e., $\langle R\rangle^F>\langle R\rangle^0$ being stretched due to the attraction of the EDMF thereby lowering their energy. The states for ν

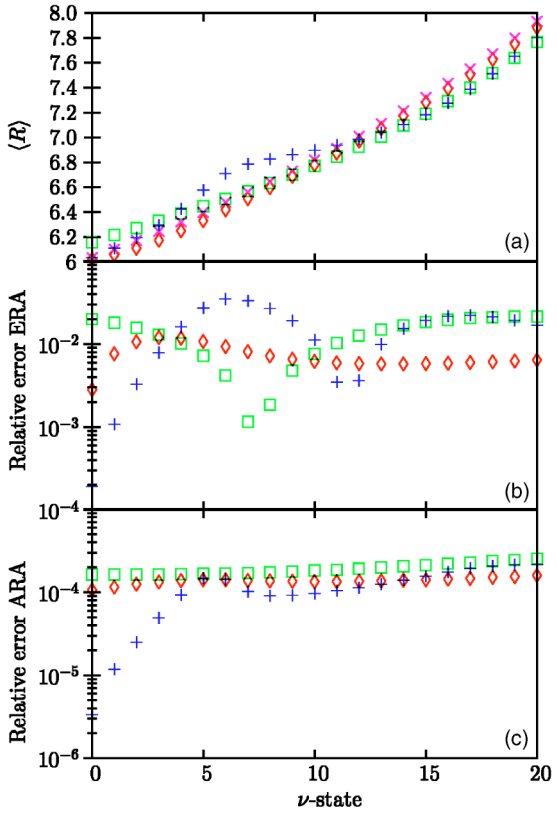

FIG. 5. (Color online) (a) The expectation values $\langle R\rangle$, (b) the relative error $\Delta\langle R\rangle_\nu^{\mathcal{E}}$ of the effective rotor approximation, (c) the relative error $\Delta\langle R\rangle_\nu^{\mathcal{A}}$ of the adiabatic rotor approximation as a function of the vibrational label $0\leqslant\nu\leqslant 20$ for states emerging from $J=0$ for $F=0$ for the Morse potential with $R_e=6.0$ a.u. and the three EDMFs D_C ($\diamond$), D_S (+), and D_W ($\square$). For completeness the field-free values of $\langle R\rangle$ ($\times$) have also been included.

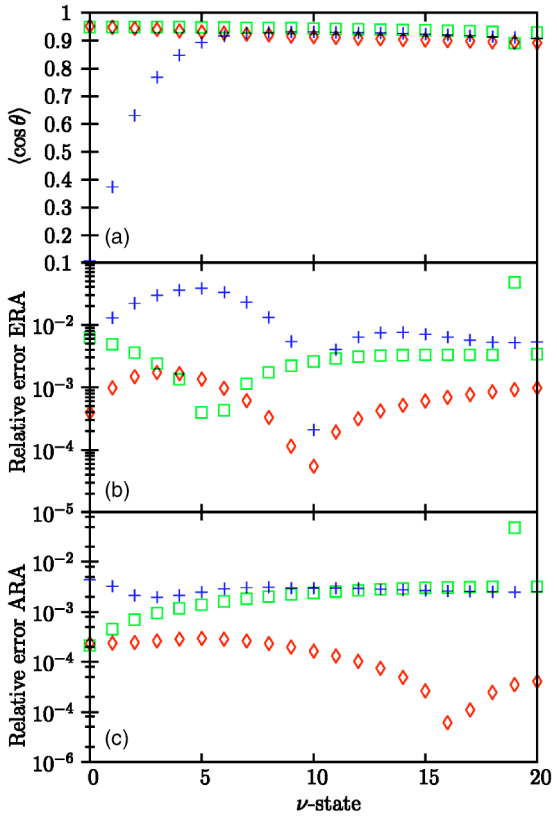

FIG. 6. (Color online) Same as in Fig. 3 but for $R_e=2.2$ a.u.

$=12-20$ possess $\langle R\rangle^F<\langle R\rangle^0$ being also attracted by the maximum of the EDMF. However, for these states a significant part of their amplitude is at distances larger than 8 a.u. and that is why they are squeezed compared to their field-free extension. A similar behavior is observed when D_W is used. The states for $\nu=0-6$ are stretched compared to their field-free counterparts. For the states $\nu=7-9$ we have $\langle R\rangle^F\approx\langle R\rangle^0$. Due to the attraction of the EDMF maximum, the states with $\nu\geqslant 10$ are again squeezed. We would like to point out the importance of these results: they show how the electric field is affecting the vibrational part of the wave function of the molecule. Indeed, we can identify this effect as an adiabatic coupling between the vibrational and rotational motion induced by the strong electric field. Figures 5(b) and 5(c) show the relative error of $\langle R\rangle$ computed by using ERA and ARA, $\Delta\langle R\rangle_\nu^{\mathcal{E}}$ and $\Delta\langle R\rangle_\nu^{\mathcal{A}}$, respectively, as a function of ν for the three EDMFs. Comparing these two figures, the ARA approximates much more accurately the FRV results than the ERA does. Only for a few states does the ERA provide an adequate description of the effects of the electric field.

B. Morse potential for $R_e=2.2$ a.u.

Figure 6(a) shows the expectation values $\langle\cos\theta\rangle$ for the states $0\leqslant\nu\leqslant 20$ emerging from the states with $J=0$ for $F=0$ for the Morse potential with $R_e=2.2$ a.u. Results for the three Gaussian EDMFs D_S, D_C, and D_W are included. The relative errors obtained by using the ERA and the ARA, $\Delta\langle\cos\theta\rangle_\nu^{\mathcal{E}}$ and $\Delta\langle\cos\theta\rangle_\nu^{\mathcal{A}}$, are presented in Figs. 6(b) and 6(c), respectively. For D_C all the states exhibit a strong orientation, which smoothly decreases as the degree of excitation increases, from $\langle\cos\theta\rangle=0.9526$ for $\nu=0$ to $\langle\cos\theta\rangle=0.8926$ for the $\nu=20$ state. For D_S the low-lying states show a weak orientation such as $\langle\cos\theta\rangle=0.1092$ for $\nu=0$. The orientation quickly increases with increasing ν, reaches a maximum for $\nu=9$ with $\langle\cos\theta\rangle=0.9312$ and slowly decreases thereafter. The orientation of the states belonging to D_W increases from $\nu=0$ to $\nu=2$ with $\langle\cos\theta\rangle=0.9485$ decreases slowly thereafter, except for the state $\nu=19$ with $\langle\cos\theta\rangle=0.8910$ for which a dip of this expectation value with respect to the values of the neighboring levels is observed. The corresponding expectation values provided by the ERA for D_C [see Fig. 6(b)] agree well with the exact ones $\Delta\langle\cos\theta\rangle_\nu^{\mathcal{E}}<0.01$. Similar results are found for D_W except again for the $\nu=19$ state $\Delta\langle\cos\theta\rangle_{19}^{\mathcal{E}}\approx 0.05$, which interrupts the smooth behavior of the ERA relative error for the other states. For D_S only the states with $\nu=2-8$ show a relative difference larger than 0.01. In Fig. 6(c) we observe how the ARA improves the results of the ERA and apart from a few exceptions we always find $\Delta\langle\cos\theta\rangle_\nu^{\mathcal{E}}>\Delta\langle\cos\theta\rangle_\nu^{\mathcal{A}}$. The ARA relative error obtained for the $\nu=19$ state using D_W is $\Delta\langle\cos\theta\rangle_{19}^{\mathcal{A}}\approx 0.05$ being much larger than the relative error for the remaining states.

Figures 7(a)–7(c) illustrate the behavior of $\langle\mathbf{J}^2\rangle$, $\Delta\langle\mathbf{J}^2\rangle_\nu^{\mathcal{E}}$, and $\Delta\langle\mathbf{J}^2\rangle_\nu^{\mathcal{A}}$, respectively, as a function of ν for the same set

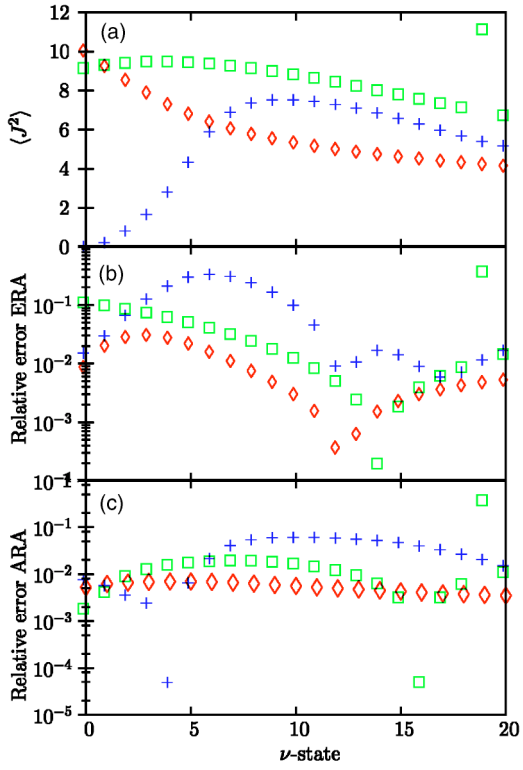

FIG. 7. (Color online) Same as in Fig. 4 but for R_e=2.2 a.u.

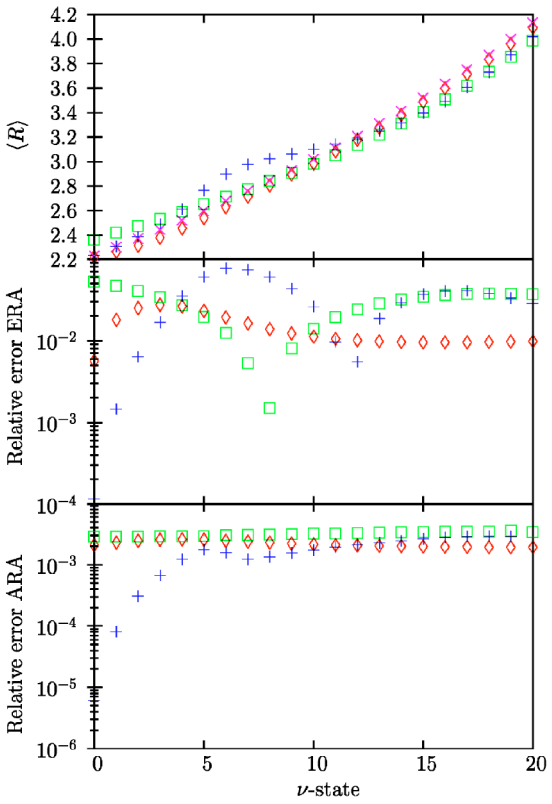

FIG. 8. (Color online) Same as in Fig. 5 but for R_e=2.2 a.u.

of states and the three EDMFs. The hybridization of this model system is much smaller than the hybridization achieved by the Morse potential with R_e=6 a.u. due to its smaller rotational constant. For D_C, $\langle \mathbf{J}^2 \rangle$ decreases as ν is increased, from $\langle \mathbf{J}^2 \rangle$=10.049 for ν=0 to $\langle \mathbf{J}^2 \rangle$=4.163 for ν=20. For the D_S we obtain a small hybridization for low-lying states, $\langle \mathbf{J}^2 \rangle$=0.018 for the rovibrational ground state, and strong mixing of the rotational motion for the states $\nu \geqslant 3$, $\langle \mathbf{J}^2 \rangle$ increases with increasing ν, reaching a maximum for ν=10 with $\langle \mathbf{J}^2 \rangle$=7.523, and decreasing thereafter. For D_W first $\langle \mathbf{J}^2 \rangle$ slightly increases with ν, reaches a maximum for the ν=5 state with $\langle \mathbf{J}^2 \rangle$=9.473, and decreases as the degree of excitation is further increased. As for the expectation value $\langle \cos\theta \rangle$, the ν=19 state shows an anomalous behavior, having a larger $\langle \mathbf{J}^2 \rangle$ than the rest of the neighboring states: $\langle \mathbf{J}^2 \rangle$=11.128. The relative error of the ERA for D_C for $1 \leqslant \nu \leqslant 10$ and ν=20 yields $\Delta\langle \mathbf{J}^2 \rangle_\nu^{\mathcal{E}} > 0.01$. For D_S we find that only the states ν=12, 16, 17, and 18 satisfy $\Delta\langle \mathbf{J}^2 \rangle_\nu^{\mathcal{E}} < 0.01$. For the states $3 \leqslant \nu \leqslant 9$ we encounter an error being larger than 0.1. In the case of D_W we see that only the states with $11 \leqslant \nu \leqslant 18$ possess $\Delta\langle \mathbf{J}^2 \rangle_\nu^{\mathcal{E}} < 0.01$. Again the state ν=19 is exceptional with $\Delta\langle \mathbf{J}^2 \rangle_{19}^{\mathcal{E}} \approx 0.37$. The ARA relative errors, see Fig. 7(c), improve in most cases but not always the results obtained by the ERA. For the state ν=19 for D_W we find a large relative error $\Delta\langle \mathbf{J}^2 \rangle_{19}^{\mathcal{A}} \approx 0.37$.

The expectation value $\langle R \rangle$, the relative errors $\Delta\langle R \rangle_\nu^{\mathcal{E}}$ and $\Delta\langle R \rangle_\nu^{\mathcal{A}}$ of the ERA and ARA are shown as a function of ν in Figs. 8(a)–8(c), respectively. By comparing Figs. 5(a) and 8(a) we conclude that the behavior of $\langle R \rangle$ for the three EDMF is similar for the two cases R_e=2.2 a.u. and R_e=6 a.u. This holds both for the dependence of $\langle R \rangle$ on the vibrational excitation and on the choice of the EDMF. Moreover, the phenomenon of squeezing and stretching of the vibrational wave function can be observed equally for R_e=2.2 a.u. We remark that the behavior of $\langle R \rangle$ as a function of ν is smooth *for all the levels* and any EDMF. The comparison of the relative errors of the ERA and ARA support our previous observation that the ARA is superior to the ERA.

Let us comment on the anomalous behavior of the expectation values $\langle \mathbf{J}^2 \rangle$ and $\langle \cos\theta \rangle$ for the state ν=19 when compared to its neighboring states. Closely inspecting higher rotational excitations it turns out that the state emerging from the field-free state with ν=18, J=3, M=0 comes very close in energy to the considered ν=19 state. For the field strength $F=10^{-3}$ a.u. the energetical spacing of these two states is very small $\Delta E = |E_{(19,0)} - E_{(18,3)}| \approx 5 \times 10^{-8}$. For F=0 these two states would not interact. However, we conjecture that the electric field induces a strong nonadiabatic mixing between these two states belonging to two different vibrational bands thereby causing the observed uncommon properties. To study this phenomenon goes however beyond the scope of the present investigation.

Comparing the relative errors obtained for $\langle \mathbf{J}^2 \rangle$ and $\langle \cos\theta \rangle$, one realizes that the latter expectation value is normally better described by the ERA and ARA than $\langle \mathbf{J}^2 \rangle$. $\langle \mathbf{J}^2 \rangle$ provides a measure for the error we perform in our approximate approaches, since the computation of it in these schemes neglects the elements (6). Therefore we can consider it as an indicator of the quality of the eigenfunctions computed within a certain approximation. We also conclude

that the adiabatic rotor approach works better for the Morse potential with $R_e=6$ a.u. compared to the system with $R_e=2.2$ a.u. We believe that the reason herefore is the separation of the vibrational and rotational energy scales. For the Morse with $R_e=6$ a.u. the ratio of the rotational and vibrational spacing is one order of magnitude smaller compared to the Morse with $R_e=2.2$ a.u. (see Fig. 1).

C. Probability densities

From the many data obtained within the present investigation let us show some representative examples for the field-induced changes introduced in the rovibrational probability densities. We compare the exact FRV results with the results of the ARA and the ERA for three typical states for a certain EDMF. As already discussed in Sec. II the ERA employs the field-free vibrational wave function whereas the ARA takes into account the adiabatic coupling of the rotational and vibrational motions.

First we consider the rovibrational ground state for the Morse potential with $R_e=6$ a.u. and the centered EDMF. Figures 9(a)–9(c) show contour plots in the (R,θ) plane of the square of the wave function computed with FRV, ARA, and ERA, respectively. The orientation achieved for this state is $\langle\cos\theta\rangle=0.983$. The position of the maximum of the wave function for $F=0$ at $R=6.02$ a.u. for $\theta=0$ is slightly modified by the electric field to $R=6.01$ a.u. and this is reproduced by the ARA. The value at the maximum $R=6.01$, $\theta=0$ for the FRV probability density is $|\Psi(6.01,0)|^2=4.90$ being reproduced by the ARA with $|\Psi(6.01,0)|^2=4.90$. However, the ERA provides a lower value $|\Psi(6.02,0)|^2=4.25$. This effect can be seen in Figs. 9(a)–9(c). The ERA wave function is vibrationally more extended than the FRV wave function, i.e., we observe a compression due to the field. The ARA reproduces this effect, which is again a manifestation of the field induced adiabatic coupling between the vibrational and rotational motions.

As a second example we analyze the rovibrational ground state of the Morse potential with $R_e=2.2$ a.u. for D_W. The contour plots of the probability densities for the FRV, ERA, and ARA are presented in Figs. 10(a)–10(c), respectively. As in the previous case the wave function is strongly oriented along the field direction, $\langle\cos\theta\rangle=0.948$. The ARA wave function provides a good approximation to the FRV one, whereas major discrepancies are observed in case of the ERA wave function. The maximum of the density for $\theta=0$ is now at $R=2.36$ a.u., i.e., due to the attraction of the EDMF it has been shifted from its field-free position $R=2.22$ a.u. The ARA yields $R=2.34$ a.u., whereas the ERA provides the field-free value. In addition, the ERA yields for the maximum $|\Psi(2.22,0)|^2=1.27$, compared to the full rovibrational result $|\Psi(2.36,0)|^2=1.37$, while the ARA gives a much better approximation $|\Psi(2.34,0)|^2=1.38$. This effect can be also observed in Figs. 10(a) and 10(c).

As a last example we present the state emerging from the field-free vibrational quantum number $\nu=5$ and the rotational quantum number $J=0$ for the Morse with $R_e=2.2$ a.u. and the shifted EDMF. The contour plots of the probability densities for the FRV, ARA, and ERA are included in Figs. 11(a)–11(c), respectively. Compared to the two above analyzed states, this state shows a weaker orientation $\langle\cos\theta\rangle=0.894$. The probability density possesses six maxima. We will concentrate here on the most pronounced one with the largest value for R. In the field-free case, this maximum is at $R=3.31$ a.u. In the presence of the electric field, the FRV analysis yields $R=3.46$ a.u., i.e., the wave function, attracted by the maximum EDMF shifted at $R=8$ a.u., is shifted towards larger values of the vibrational coordinate. Using the ARA we obtain $R=3.44$ a.u., which is a very good approximation to the exact result. Here the maximal density is $|\Psi(3.46,0)|^2=0.4$ being slightly overestimated by the ARA result $|\Psi(3.44,0)|^2=0.42$. For the ERA we obtain a much lower value, $|\Psi(3.31,0)|^2=0.31$. In addition, the ERA is also not able to reproduce the extension of

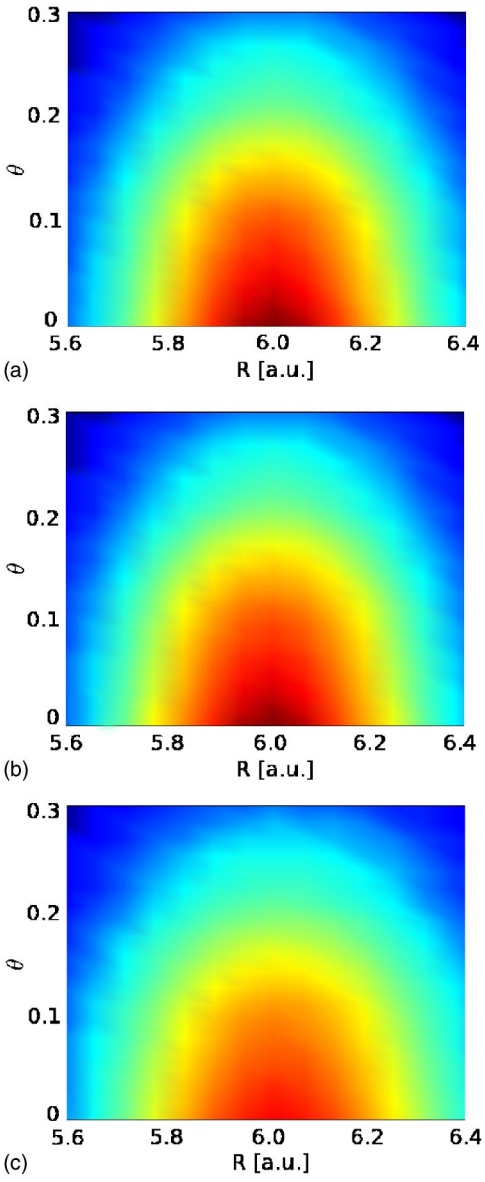

FIG. 9. (Color online) Probability density of the rovibrational ground state of the Morse potential with $R_e=6.0$ a.u. and the centered EDMF for the field strength $F=10^{-3}$ a.u.

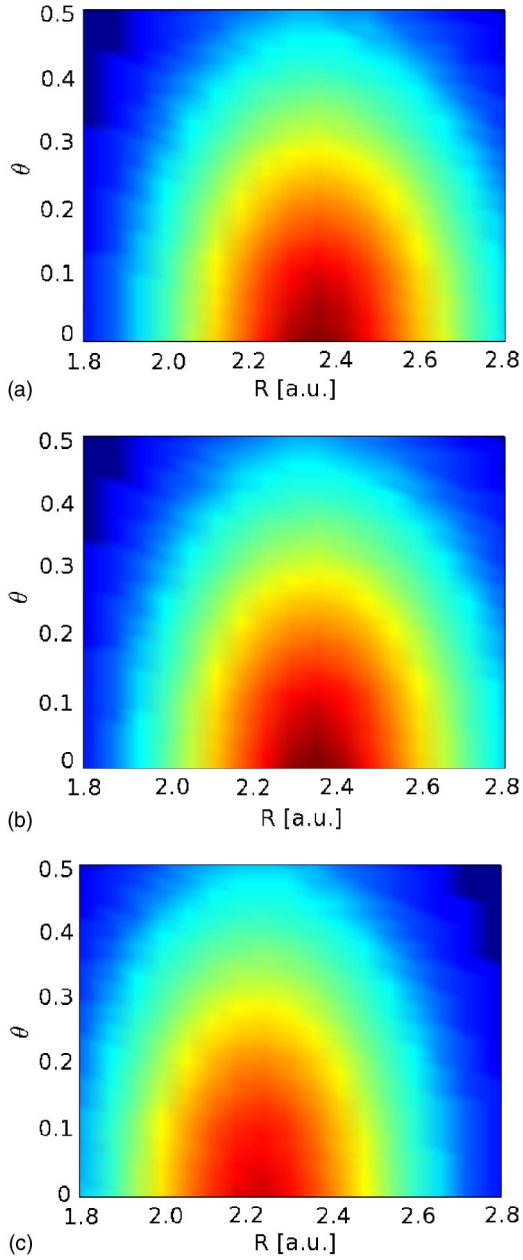

FIG. 10. (Color online) Probability density of the rovibrational ground state of the Morse potential with $R_e=2.20$ a.u. and D_W for the field strength $F=10^{-3}$ a.u.

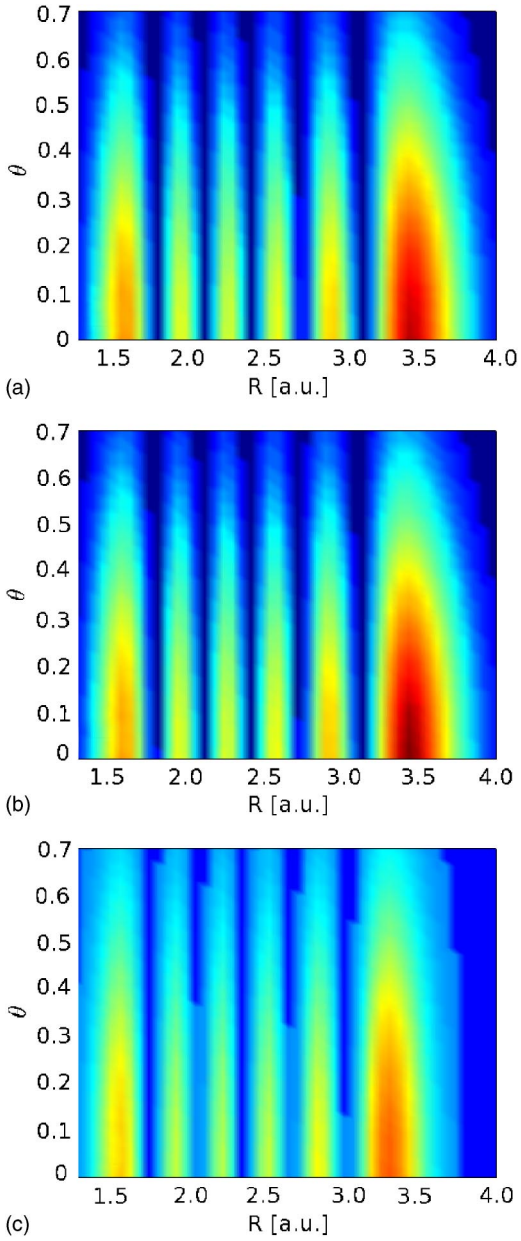

FIG. 11. (Color online) Probability density of the state $\nu=5$ emerging from the field-free $J=0$ state of the Morse potential with $R_e=2.20$ a.u. and D_S for the field strength $F=10^{-3}$ a.u.

each hump of the wave function, see Fig. 11(c) compared to Fig. 11(a).

V. SUMMARY AND OUTLOOK

The rovibrational motion of diatomic molecules is given by a product of a (J-dependent) vibrational and a rotational wave function (many of the Coriolis coupling terms vanish in case of an electronic ground state of $^1\Sigma^+$ symmetry and we neglect the remaining ones). In the presence of a static homogeneous electric field that is weak enough to be treated perturbatively with respect to the electronic structure of the molecule but strong enough to act nonperturbatively on its nuclear motion this separability is no longer present. Still, for not too strong fields and/or rigid molecules, i.e., molecules for which the energy scales of the vibrational and rotational motions are well separated, the dominant effect of the electric field is to hybridize the rotational motion. The effective rotor approximation developed in a previous work of the authors describes this hybridization accurately and in particular it provides the correct description of the angular motion depending on the vibrational state. Here the vibrational motion is assumed to be not influenced by the electric field. In contrast to this the traditional pendular state approach provides a hybridization that is independent of the vibrational state.

In the present work we made a step beyond the above-described regime and investigated stronger fields and/or flop-

pier systems. Since we are interested in new phenomena and properties we did not address a specific molecule, i.e., potential-energy curve and electric dipole moment function, but a model—the Morse potential—possessing variable parameters and we study three models for the electronic dipole moment function covering typical cases. The field strength we have been using $F=10^{-3}$ a.u. corresponding to 514 (MV/m) is somewhat above the experimentally accessible static field strength. However, we expect that the principal effects we have found do occur in certain regimes and species at significantly lower field strengths. Moreover, our results should be equally applicable to the quasistatic regime of low-frequency electromagnetic fields for which the dynamical and electromagnetic frequency scales are well separated. An estimation of the (semiclassical) tunneling rate due to the presence of the field $F=10^{-3}$ a.u. indicates that the electronic ionization process can safely be neglected. Furthermore, in many cases the interaction with the field due to the polarizability of the molecule can equally be neglected due to its quadratic dependence on the field strength.

Starting from the rovibrational equation of motion in the molecule fixed frame we have developed an adiabatic separation of the vibrational and rotational motions. It turns out that the effective rotor approximation is a crude adiabatic approach in this framework: the fast vibrational motion is the field-free one and in particular independent on the slow dynamical variable, i.e., the angular motion. We established the full adiabatic approximation, the so-called adiabatic rotor approach, to the rovibrational motion for which the vibrational wave function depends parametrically on the angular variable. Subsequently studies for several model systems including many vibrational excitations have been performed. Our focus has been on the states emerging from the field-free ground rotational states $J=0$ for $M=0$. It turns out that applying the above field strength we indeed enter the regime where the ERA description is no longer adequate and field-induced effects and full adiabaticity occur. The ARA accurately describes the energies and physical properties, i.e., total wave functions in this regime. We have analyzed the orientation effects, the mixing of angular momenta, and the vibrational stretching and squeezing effects due to the external field in detail. In the case of a shifted electric dipole moment function we observed a distortion of the wave function specifically a squeezing effect towards the maximum of the EDMF. We remark that these properties and effects depend on the state under consideration which adds to the variety of possible behavior and properties in the presence of the field.

Paradigms of heteronuclear diatomic molecules with a large equilibrium internuclear distance, a small dissociation energy, and a large maximal electric dipole moment are the alkali dimers. The latter are currently in the focus of ultracold molecular physics since they constitute the prototype of an ultracold quantum gas with long-range dipole-dipole interactions. Several experimental groups are working in this direction [41–43]. However, there is still a need for accurate potential-energy curves and electric dipole moment functions for these species, naming specifically the LiCs dimer.

The vibrational state dependence of the adiabatic rotor equation together with the field-induced adiabaticity of the vibrational and rotational motion open interesting perspectives for the application of the external field to hybridize the rovibrational motion. Natural extensions of the present work would include the investigation of the hybridization of states emerging from higher rotational excitations and/or studies of states with nonzero magnetic quantum numbers M.

ACKNOWLEDGMENTS

The authors thank H. D. Meyer and M. Weidemüller for very helpful discussions. R.G.F. gratefully acknowledges the support of the Junta de Andalucía (under the program Retorno de Investigadores a Centros de Investigación Andaluces), the Alexander von Humboldt Foundation, and financial support for traveling by Spanish Project No. BFM2001-3878-C02-01 (MCYT).

[1] S. Jochim, M. Bartenstein, A. Altmeyer, G. Hendl, S. Riedl, C. Chin, J. Hecker Denschlag, and R. Grimm, Science **302**, 2101 (2003).
[2] M. Greiner, C. A. Regal, and D. S. Jin, Nature (London) **426**, 537 (2003).
[3] M. W. Zwierlein, C. A. Stan, C. H. Schunck, S. M. F. Raupach, S. Gupta, Z. Hadzibabic, and W. Ketterle, Phys. Rev. Lett. **91**, 250401 (2003).
[4] J. L. Bohn, Phys. Rev. A **63**, 052714 (2001).
[5] R. Krems and A. Dalgarno, J. Chem. Phys. **117**, 118 (2002).
[6] K. Burnett, P. S. Julienne, P. D. Lett, E. Tiesinga, and C. J. Williams, Nature (London) **416**, 225 (2002).
[7] M. Kajita, Eur. Phys. J. D **23**, 337 (2003); **31**, 39 (2004).
[8] D. J. Heinzen, Roahn Wynar, P. D. Drummond, and K. V. Kheruntsyan, Phys. Rev. Lett. **84**, 5029 (2000).
[9] J. J. Hope and M. K. Olsen, Phys. Rev. Lett. **86**, 3220 (2001).
[10] N. Balakrishnan and A. Dalgarno, Chem. Phys. Lett. **341**, 652 (2001).
[11] E. Bodo, F. A. Gianturco, and A. Dalgarno, J. Chem. Phys. **116**, 9222 (2002).
[12] D. DeMille, Phys. Rev. Lett. **88**, 067901 (2002).
[13] D. DeMille, F. Bay, S. Bickman, D. Kawall, D. Krause, Jr., S. E. Maxwell, and L. R. Hunter, Phys. Rev. A **61**, 052507 (2000).
[14] D. Kawall, F. Bay, S. Bickman, Y. Jiang, and D. DeMille, Phys. Rev. Lett. **92**, 133007 (2004).
[15] J. K. Webb, M. T. Murphy, V. V. Flambaum, V. A. Dzuba, J. D. Barrow, C. W. Churchill, J. X. Prochaska, and A. M. Wolfe, Phys. Rev. Lett. **87**, 091301 (2001).
[16] Ch. Daussy, T. Marrel, A. Amy-Klein, C. T. Nguyen, Ch. J. Bordé, and Ch. Chardonne, Phys. Rev. Lett. **83**, 1554 (1999).
[17] H. L. Bethlem, F. M. H. Crompvoets, R. T. Jongma, S. Y. T. van de Meerakker, and G. Meijer, Phys. Rev. A **65**, 053416 (2002).

[18] H. L. Bethlem, G. Berden, and G. Meijer, Phys. Rev. Lett. **83**, 1558 (1999).
[19] Y. Yamakita, S. R. Procter, A. L. Goodgame, T. P. Softley, and F. Merkt, J. Chem. Phys. **112**, 1419 (2004).
[20] A. V. Avdeenkov and J. L. Bohn, Phys. Rev. A **66**, 052718 (2002).
[21] A. V. Avdeenkov and J. L. Bohn, Phys. Rev. Lett. **90**, 043006 (2003).
[22] P. R. Brooks, Science **193**, 11 (1976).
[23] S. Stolte, in *Atomic and Molecular Beam Methods*, edited by G. Scoles (Oxford University Press, New York, 1988), Vol. 1, Chap. 25.
[24] H. J. Loesch and A. Remscheid, J. Chem. Phys. **93**, 4779 (1990).
[25] B. Friedrich and D. R. Herschbach, Nature (London) **253**, 412 (1993).
[26] B. Friedrich, D. P. Pullman, and D. R. Herschbach, J. Phys. Chem. **95**, 8118 (1991).
[27] J. M. Rost, J. C. Griffin, B. Friedrich, and D. R. Herschbach, Phys. Rev. Lett. **68**, 1299 (1992).
[28] P. A. Block, E. J. Bohac, and R. E. Miller, Phys. Rev. Lett. **68**, 1303 (1992).
[29] B. Friedrich, H. G. Rubahn, and N. Sathyamurthy, Phys. Rev. Lett. **69**, 2487 (1992).
[30] P. Schmelcher, L. S. Cederbaum, and U. Kappes, in *Conceptual Trends in Quantum Chemistry*, edited by E. S. Kryachko and J. L. Calais (Kluwer, Dordrecht, 1994), pp. 1–51.
[31] A. Slenczka, B. Friedrich, and D. Herschbach, Phys. Rev. Lett. **72**, 1806 (1994).
[32] B. Friedrich and D. Herschbach, Phys. Rev. Lett. **74**, 4623 (1995).
[33] G. R. Kumar, P. Gross, C. P. Safvan, F. A. Rajgara, and D. Mathur, Phys. Rev. A **53**, 3098 (1996).
[34] W. Kim and P. M. Felker, J. Chem. Phys. **107**, 2193 (1997).
[35] J. Ortigoso, M. Rodríguez, M. Gupta, and B. Friedrich, J. Chem. Phys. **110**, 3870 (1999).
[36] H. Sakai, C. P. Safvan, J. J. Larsen, K. M. Hilligsøe, K. Hald, and H. Stapelfeldt, J. Chem. Phys. **110**, 10235 (1999).
[37] K. von Meyenn, Z. Phys. **231**, 154 (1970).
[38] R. Kanya and Y. Ohshimar, Phys. Rev. A **70**, 013403 (2004).
[39] R. González-Férez and P. Schmelcher, Phys. Rev. A **69**, 023402 (2004).
[40] M. Korek, A. R. Allouche, K. Fakhereddine, and A. Chaalan, Can. J. Phys. **78**, 977 (2000).
[41] C. A. Stan, M. W. Zwierlein, C. H. Schunck, S. M. F. Raupach, and W. Ketterle, Phys. Rev. Lett. **93**, 143001 (2004).
[42] S. Kotochigova, E. Tiesinga, and P. S. Julienne, Eur. Phys. J. D **31**, 189 (2004).
[43] M. Mudrich, O. Bünermann, F. Stienkemeier, O. Dulieu, and M. Weidemüller, Eur. Phys. J. D **31**, 291 (2004).